Defence Science Journal, Vol 47, No 2, April 1997, pp. 225-238

Optical Studies on Rare Earth Lasing Materials

S.P. Tandon, Y.K. Sharma, N.B. Bishnoi and K. Tandon

J.N.V. University, Jodhpur-342 001.

ABSTRACT

Neodymium-doped borate and phosphate glass specimens have been prepared by melt-quenching technique. Their absorption spectra have been recorded in the region 400 - 900 nm. From observed absorption spectra, Judd Ofelt (JO), Ω_t, parameters ($t = 2$, 4 and 6) have been computed. They have been used to calculate the laser parameters, viz., spontaneous emission probability (A), fluorescence branching ratio (β) and stimulated emission cross-section (σ). They exhibit the suitability of the present glass specimen for laser action. The effects of composition and concentration of the dopant on these parameters have been discussed. A comparative study of stimulated emission cross-section of different types of doped glasses has also been made.

1. INTRODUCTION

Nd:YAG laser were developed for high peak power[1] and high repetition frequencies[2]. Though many other lasers are now available[3,4], *Nd*:YAG lasers continue to have many applications. Since *Nd*: YAG is very expensive, search was made for a substitute for it. It is well-known that the spectroscopic properties of rare earth ions are strongly affected by glass compositions[5]. This makes it possible to tailor the host glass compositions with spectroscopic features of rare earth ions suitable for efficient laser performance. Moreover, trivalent rare earth ions present a unique opportunity for *a priori* calculations to be made from absorption and fluorescence spectra of small samples. Such predictions are very important for preparing materials based on transparent media doped with rare earth ions. The performance of glass lasers can be predicted with reasonable accuracy based on such calculations of laser parameters[6]. This avoids the preparation of large samples at the initial stage. Only small samples of Nd^{3+} doped glass specimens need to be studied.

In the present paper, the preparation, spectral properties and comparative study of predicted laser performance in borate, phosphate and other glasses doped with Nd^{3+} ions have been discussed.

2. EXPERIMENTAL DETAILS

Borate and phosphate glass specimens were prepared by melt-quenching technique[7] using the silicon-carbide furnace capable of attaining a temperature of 1450 °C, which was fabricated in the laboratory. In this furnace, the temperature is maintained by a digital electronic controller and read with the help of Pt-Rh thermocouple with a control accuracy of ±4 °C. It is lined inside with high quality alumina cement and has a hearth area of 300 cm^2. Weighed quantities of constituents were ground in an automatic mortar for 4 hr to attain homogeneity. The temperature of alumina crucible containing a small amount of the batch material was slowly raised to 300 °C and then it was maintained at this temperature till whole of the batch material had been charged into the crucible. Charging of the whole batch at a time was restricted

Received 16 May 1996, revised 30 October 1996

Table 1. Compositions (wt %) of various undoped and Nd^{3+} ion doped borate and phosphate glass specimens

Specimen code	Former	Modifier		Intermediate	Dopant	Codopant
		Primary	Secondary			
BU01	B_2O_3(75.00)		CaO(05.00)			
BD02	B_2O_3(73.78)		CaO(04.92)		Nd_2O_3(1.62)	
BD03	B_2O_3(73.66)		CaO(04.92)		Nd_2O_3(1.62)	CeO_2(0.16)
BU04	B_2O_3(48.27)			Al_2O_3(30.23)		
BD05	B_2O_3(47.50)			Al_2O_3(29.73)	Nd_2O_3(1.62)	
BU06	B_2O_3(56.00)			Al_2O_3(15.00)		
BD07	B_2O_3(55.20)			Al_2O_3(14.78)	Nd_2O_3(1.45)	
BD08	B_2O_3(54.40)			Al_2O_3(14.58)	Nd_2O_3(2.85)	
BD09	B_2O_3(55.11)			Al_2O_3(14.76)	Nd_2O_3(1.45)	CeO_2(0.14)
BU10	B_2O_3(56.00)		MgO(10.00)	Al_2O_3(05.00)		
BD11	B_2O_3(55.11)		MgO(09.84)	Al_2O_3(04.92)	Nd_2O_3(1.45)	CeO_2(0.14)
BU12	B_2O_3(56.00)		CaO(10.00)	Al_2O_3(05.00)		
BD13	B_2O_3(54.42)		CaO(09.71)	Al_2O_3(04.85)	Nd_2O_3(2.85)	
BD14	B_2O_3(55.11)		CaO(09.84)	Al_2O_3(04.92)	Nd_2O_3(1.45)	CeO_2(0.14)
BU15	B_2O_3(56.00)		BaO(10.00)	Al_2O_3(05.00)		
BD16	B_2O_3(55.11)		BaO(09.84)	Al_2O_3(04.92)	Nd_2O_3(1.45)	CeO_2(0.14)
PU17	P_2O_5(56.00)			Al_2O_3(15.00)		
PD18	P_2O_5(55.20)			Al_2O_3(14.78)	Nd_2O_3(1.45)	
PD19	P_2O_5(55.11)			Al_2O_3(14.76)	Nd_2O_3(1.45)	CeO_2(0.14)
PU20	P_2O_5(56.00)		MgO(10.00)	Al_2O_3(05.00)		
PD21	P_2O_5(55.20)		MgO(09.85)	Al_2O_3(04.92)	Nd_2O_3(1.45)	
PU22	P_2O_5(56.00)		CaO(10.00)	Al_2O_3(05.00)		
PD23	P_2O_5(55.20)		CaO(09.85)	Al_2O_3(04.92)	Nd_2O_3(1.45)	
PD24	P_2O_5(54.90)		CaO(09.80)	Al_2O_3(04.90)	Nd_2O_3(2.00)	
PD25	P_2O_5(54.82)		CaO(09.78)	Al_2O_3(04.88)	Nd_2O_3(2.14)	
PD26	P_2O_5(54.73)		CaO(09.78)	Al_2O_3(04.88)	Nd_2O_3(2.14)	$BiCl_3$(0.14)
PD27	P_2O_5(54.58)		CaO(09.95)	Al_2O_3(04.86)	Nd_2O_3(2.14)	$BiCl_3$(0.42)
PU28	P_2O_5(56.00)		BaO(10.00)	Al_2O_3(05.00)		
PD29	P_2O_5(55.20)		BaO(09.85)	Al_2O_3(04.92)	Nd_2O_3(1.45)	
PD30	P_2O_5(54.42)		BaO(09.71)	Al_2O_3(04.85)	Nd_2O_3(2.85)	
PD31	P_2O_5(55.11)		CaO(09.84)	Al_2O_3(04.92)	Nd_2O_3(1.45)	CeO_2(0.14)

BU : Undoped borate glass specimen
BD : Doped borate glass specimen
PU : Undoped phosphate glass specimen
PD : Doped phosphate glass specimen

due to evolution of CO_2 and water vapours resulting in excessive frothing. After the whole batch material had attained a temperature of 300 °C, the crucible was further heated to a

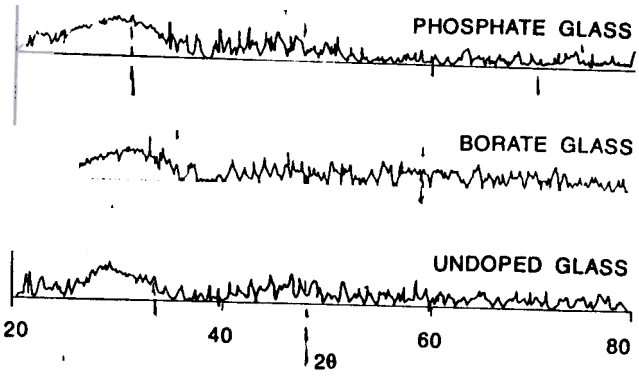

Figure 1. X-ray diffractogram of undoped and neodymium doped borate and phosphate glass specimens.

working temperature of 900 °C for phosphate glasses and 1000 °C for borate glasses. The working temperature was maintained for 5 hr to ensure the melt to be free from gases. Before pouring, the melt was stirred several times to ensure homogeneity. The melt was quickly poured into the graphite mould fitted on a heavy copper block. The specimen was then removed from the mould and kept for annealing in Therelak furnace at 10 - 20 °C above softening temperature so as to remove stresses and give thermal stability and strength to the specimen. The glass samples were polished using cerium oxide powder. They were again annealed for 2 hr to remove mechanical stresses, which might have developed during lapping and polishing. The final compositions of the borate and phosphate glass specimens are given in Table 1. Glass specimens contain no crystalline phases as revealed by X-ray diffractograms. A representative diffractogram is given in Fig. 1.

The absorption spectra were recorded using 'Hitachi' fluorescence spectrophotometer model-3000 in both scan modes in the wavelength range 400-800 nm. Absorption spectra in the region 800-900 nm were measured on Carl Zeiss Jena spectrophotometer model 'VSU-2P'. The densities of glass specimens were measured by displacement method using A.R. grade benzene and sensitive single pan balance reading correct up to 10^{-4} g. The refractive indices of the glass specimens were determined using Abbe refractometer.

Table 2. Physical properties of various undoped and Nd^{3+} ion doped borate and phosphate glass specimens

Specimen code	Thickness (cm)	Density (g/cm^3)	Mean refractive index
BU01	0.355	2.380	1.579
BD02	0.420	2.575	1.585
BD03	0.415	2.591	1.583
BU04	0.273	2.308	1.559
BD05	0.325	2.330	1.562
BU06	0.382	2.408	1.569
BD07	0.316	2.435	1.571
BD08	0.399	2.454	1.575
BD09	0.336	2.441	1.575
BU10	0.371	2.470	1.576
BD11	0.351	2.486	1.578
BU12	0.382	2.519	1.577
BD13	0.380	2.545	1.581
BD14	0.334	2.539	1.580
BU15	0.345	2.624	1.581
BD16	0.408	2.639	1.583
PU17	0.404	2.681	1.513
PD18	0.395	2.696	1.515
PD19	0.402	2.699	1.514
PU20	0.406	2.702	1.517
PD21	0.370	2.720	1.518
PU22	0.341	2.752	1.521
PD23	0.351	2.781	1.525
PD24	0.375	2.796	1.526
PD25	0.275	2.809	1.528
PD26	0.325	2.812	1.531
PD27	0.374	2.814	1.533
PU28	0.325	2.911	1.538
PD29	0.333	2.927	1.539
PD30	0.301	2.949	1.141
PD31	0.330	2.934	1.140

3. RESULTS & DISCUSSION

The physical properties of glass specimens are given in Table 2. Representative absorption spectra of Nd^{3+} ion in borate and phosphate glasses are shown in Fig. 2. Nine bands have been observed in the region 400-900 nm. It is important to note that

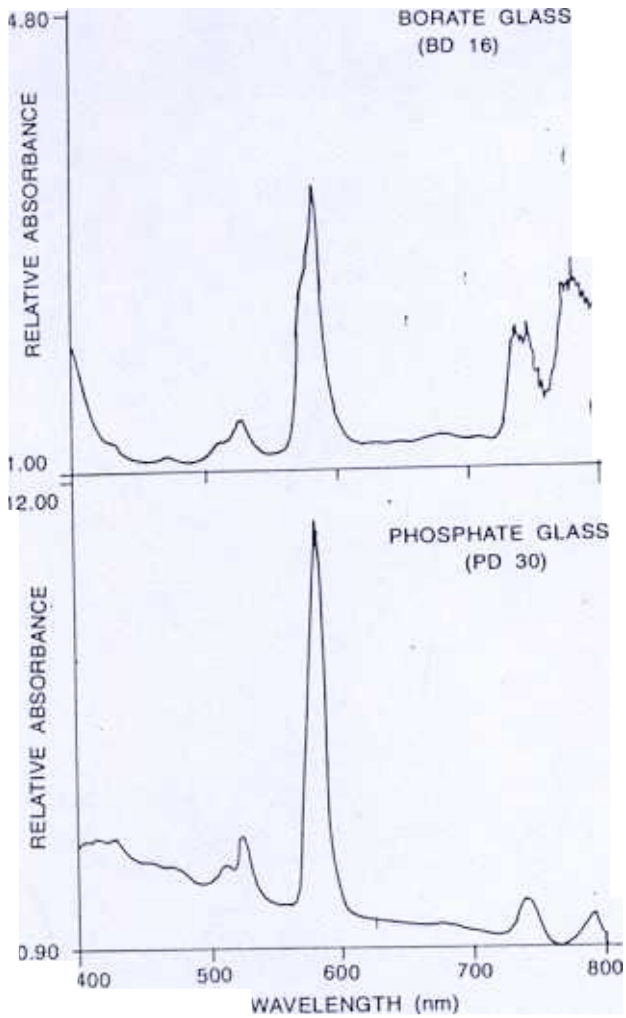

Figure 2. Absorption spectra of borate and phosphate glass specimens.

the second derivative spectrum (Fig. 3) reveals that the bands appearing at 746, 583 and 462 nm are composite in nature. Consequently, their intensities have been considered to be due to the transitions from ground state $^4I_{9/2}$ to ($^4F_{7/2}$ and $^4S_{9/2}$), $^4I_{9/2}$ to ($^4G_{5/2}$ and $^2G_{7/2}$), and $^4I_{9/2}$ to $(^2D,^2P)_{3/2}$ respectively. The mean peak values of the absorption bands and line strengths for the observed bands have been computed from their integrated intensity and their values are collected in Tables 3 and 4. The observed energies and line strengths of bands can be used for calculation of interaction and Judd-Ofelt parameters, respectively.

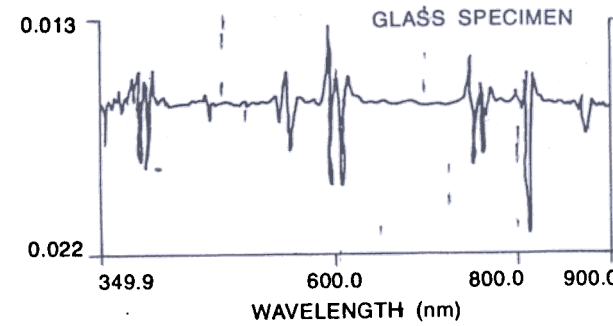

Figure 3. Second derivative spectrum of glass specimen

3.1 Energy Interaction Parameters

The energy E_j can be expressed in terms of interaction parameters - (Slater-Condon) F_k's and (Lande) ξ_{4f} by Taylor series expansion for a small variation of energies ΔE_j . In the first order approximation, the energy E_j of the jth level is given by[8,9]

$$E_j(F_k, \xi_{4f}) = E_{oj}(F_k, \xi_{4f}) + \sum_{k=2,4,6} \frac{\partial E_j}{\partial F_k} \Delta F_k + \frac{\partial E_j}{\partial \xi_{4f}} \Delta \xi_{4f} \quad (1)$$

where

E_{oj} is the zero order energy of jth level and ΔF_k and $\Delta\xi_{4f}$ are the small changes in the corresponding parameters. The values of zero order energy (E_{oj}) and partial derivatives $\partial E_j/\partial F_k$ and $\partial E_j/\partial \xi_{4f}$ for the observed levels of Nd^{3+} ions calculated by Wong[8] have been used.

The F_k and ξ_{4f} parameters are then evaluated using equations

$$F_k = F_k^o + \Delta F_k \quad (2)$$

$$\xi_{4f} = \xi_{4f}^o + \Delta \xi_{4f} \quad (3)$$

where

F_k^o and ξ_{4f}^o are the zero order values[9] of the parameters F_k and ξ_{4f}, respectively. The computed values of F_k and ξ_{4f} parameters have been computed using strong peaks due to transitions to $^4F_{3/2}$, $^4F_{5/2}$, $^4F_{7/2}$, $^4G_{5/2}$, $^4G_{7/2}$, $^4G_{9/2}$, $^2G_{9/2}$ and

Table 3. Experimental and calculated line strengths 'S' of Nd^{3+} ion in borate glass specimens

Bands	BD02 Wave-length (nm)	BD02 S(pm^2) Expt.	BD02 S(pm^2) Cal.	BD03 Wave-length (nm)	BD03 S(pm^2) Expt.	BD03 S(pm^2) Cal.	BD05 Wave-length (nm)	BD05 S(pm^2) Expt.	BD05 S(pm^2) Cal.	BD07 Wave-length (nm)	BD07 S(pm^2) Expt.	BD07 S(pm^2) Cal.	BD08 Wave-length (nm)	BD08 S(pm^2) Expt.	BD08 S(pm^2) Cal.
$^4F_{3/2}$	875.0	1.216	1.047	875.0	1.218	1.017	875.0	1.238		875.0	1.229	1.081	875.0	1.226	1.355
$^2H_{9/2},^4F_{5/2}$	803.0	3.728	3.222	803.0	3.733	3.291	803.0	3.794		803.0	3.768	3.342	803.0	3.757	3.595
$^4S_{3/2},^4F_{7/2}$	743.4	3.338	3.114	748.6	3.697	3.269	735.0	3.173		740.0	3.315	3.268	740.6	3.330	3.276
$^4F_{9/2}$	681.2	1.064	0.225	680.6	1.058	0.232	682.2	1.300		684.2	0.572	0.233	682.6	0.404	0.241
$^4H_{11/2}$	625.4	0.305	0.056	628.0	0.090	0.058	625.0	0.230		631.4	0.361	0.059	628.4	0.092	0.061
$^2G_{7/2},^4G_{5/2}$	582.2	9.811	9.288	582.4	8.579	8.151	582.4	11.855		584.0	7.648	7.431	584.0	7.457	7.358
$^2K_{13/2},^4G_{7/2}$	524.8	1.796	1.386	525.0	2.193	1.300	525.2	2.517		526.8	0.987	1.287	526.6	1.882	1.422
$^4G_{9/2}$	511.6	1.006	0.427	511.2	1.253	0.420	512.0	1.690		512.8	1.022	0.433	512.6	1.041	0.207
$^2K_{15/2}, ^2G_{9/2}$	473.6	0.530	0.203	473.8	0.565	0.205	475.2	1.046		475.8	0.291	0.209	474.0	0.287	0.231
$^4G_{11/2},(^2D^2P)_{3/2}$	458.2	0.136	0.120	455.6	0.333	0.118	461.4	0.731		461.2	0.184	0.125	461.2	0.167	0.153
$^2P_{1/2},^2D_{5/2}$	428.6	0.605	0.138	428.6	0.564	0.132	430.2	0.438		430.4	0.358	0.142	430.4	0.119	0.186
Goodness of fit		0.275			0.390			0.854			0.119			0.124	
		BD09			BD11			BD13							
$^4F_{3/2}$	875.0	1.226	1.124	875.0	1.223	1.203	875.0	1.220	1.330	875.0		1.086	875.0		1.059
$^2H_{9/2},^4F_{5/2}$	803.0	3.757	3.505	803.0	3.748	3.486	803.0	3.739	3.613	803.0		3.502	803.0		3.593
$^4S_{3/2},^4F_{7/2}$	741.0	3.406	3.452	742.8	3.552	3.320	741.6	3.243	3.319	756.2		3.502	745.0		3.659
$^4F_{9/2}$	683.0	0.705	0.245	682.2	0.269	0.239	684.2	0.288	0.244	681.4		0.247	687.2		0.257
$^4H_{11/2}$	628.4	0.237	0.062	627.2	0.033	0.060	625.6	0.095	0.062	631.4		0.062	628.0		0.065
$^2G_{7/2},^4G_{5/2}$	583.8	7.100	7.011	584.2	7.462	7.239	584.6	8.435	8.428	584.6		6.658	584.8		7.164
$^2K_{13/2},^4G_{7/2}$	526.2	1.023	1.297	526.6	1.828	1.340	527.4	1.432	1.480	526.8		1.260	527.8		1.291
$^4G_{9/2}$	512.2	0.468	0.469	513.4	0.672	0.463	513.2	0.713	0.500	513.0		0.439	514.0		0.442
$^2K_{15/2}, ^2G_{9/2}$	474.4	0.189	0.219	474.4	0.254	0.220	476.2	0.183	0.231	473.6		0.217	474.4		0.222
$^4G_{11/2},(^2D^2P)_{3/2}$	457.4	0.056	0.130	458.2	0.434	0.137	463.2	0.055	0.151	457.6		0.126	457.6		0.124
$^2P_{1/2},^2D_{5/2}$	430.2	0.267	0.147	430.2	1.052	0.161	431.8	0.248	0.181	430.4		0.140	428.4		0.135
Goodness of fit		0.053			0.167			0.012							

$^2D_{5/2}$ levels for one specimen each of borate and phosphate glasses and are presented in Table 5. These parameters can also be evaluated empirically[10] using the expressions

$$F_2 = 12.4\ (Z\text{-}34) \tag{4}$$

$$\xi_{4f} = 142\ Z - 7648 \tag{5}$$

where

Z is the atomic number of the rare earth ion. The empirical values of F_2 and ξ_{4f} are 322.4 and 858 cm^{-1}, respectively. These values are in close agreement with the respective experimental values (Table 5). Nephelauxetic ratio[11] (β) and bonding parameter[11] ($b^{1/2}$) can be calculated from F_2 values. Their values are given in Table 5. They reveal covalent nature of the glass specimens under study.

Racah parameters (E^k) have been deduced from F_k parameters[12] (Table 5). The ratios of Racah parameters E^1/E^3 and E^2/E^3 are about 10 and 0.05 respectively, which are almost equal to the hydrogenic ratio[10]. This implies that Nd^{3+} ions at different doping concentrations are subjected to similar force fields.

3.2 Judd-Ofelt Intensity Parameters

The observed intensities of the absorption bands of rare earth ions were explained by Judd[13]

Table 4. Experimental and calculated line strengths 'S' of Nd^{3+} ion in phosphate glass specimens

Bands	PD18 Wave-length (nm)	PD18 S(pm^2) Expt.	PD18 S(pm^2) Cal.	PD19 Wave-length (nm)	PD19 S(pm^2) Expt.	PD19 S(pm^2) Cal.	PD21 Wave-length (nm)	PD21 S(pm^2) Expt.	PD21 S(pm^2) Cal.	PD23 Wave-length (nm)	PD23 S(pm^2) Expt.	PD23 S(pm^2) Cal.	PD24 Wave-length (nm)	PD24 S(pm^2) Expt.	PD24 S(pm^2) Cal
$^4F_{3/2}$	875.0	1.481	1.551	875.0	1.483	1.624	875.0	1.487	1.491	875.0	1.470	1.459	875.0	1.469	1.461
$^2H_{9/2},^4F_{5/2}$	803.0	4.318	3.977	803.0	4.325	4.079	803.0	4.337	3.943	803.0	4.286	4.062	803.0	4.283	4.005
$^4S_{3/2},^4F_{7/2}$	739.2	3.359	3.420	739.6	3.503	3.612	741.8	3.720	3.547	738.6	3.807	3.803	738.6	3.861	3.730
$^4F_{9/2}$	683.4	0.500	0.264	683.4	0.461	0.272	681.6	0.407	0.215	684.0	0.462	0.276	682.0	0.596	0.271
$^4H_{11/2}$	628.8	0.118	0.065	630.0	0.089	0.053	626.4	0.299	0.067	628.2	0.098	0.070	629.0	0.080	0.069
$^2G_{7/2},^4G_{5/2}$	584.0	10.752	10.612	583.8	7.960	7.917	582.6	11.173	10.915	582.8	7.934	7.832	583.2	7.827	7.628
$^2K_{13/2},^4G_{7/2}$	526.8	1.754	1.738	526.4	1.596	1.620	525.8	2.206	1.738	525.6	1.479	1.547	525.8	1.983	1.529
$^4G_{9/2}$	513.8	0.839	0.568	513.4	0.877	0.582	512.6	1.299	0.560	512.8	0.922	0.549	512.8	1.046	0.545
$^2K_{15/2}, ^2G_{9/2}$	476.0	0.703	0.254	476.6	0.299	0.264	475.6	0.533	0.254	474.0	0.442	0.258	476.8	0.546	0.255
$^4G_{11/2},(^2D^2P)_{3/2}$	461.4	0.279	0.174	462.2	0.204	0.183	462.6	0.385	0.168	459.2	0.128	0.166	462.4	0.334	0.166
$^2P_{1/2},^2D_{5/2}$	431.4	0.227	0.217	430.6	0.158	0.227	430.6	0.387	0.206	431.0	0.277	0.198	430.6	0.244	0.199
Goodness of fit		0.061			0.028			0.158			0.035			0.101	

Bands	PD25 Wave-length (nm)	PD25 S(pm^2) Expt.	PD25 S(pm^2) Cal.	PD26 Wave-length (nm)	PD26 S(pm^2) Expt.	PD26 S(pm^2) Cal.	PD27 Wave-length (nm)	PD27 S(pm^2) Expt.	PD27 S(pm^2) Cal.	PD29 Wave-length (nm)	PD29 S(pm^2) Expt.	PD29 S(pm^2) Cal.	PD30 Wave-length (nm)	PD30 S(pm^2) Expt.	PD30 S(pm^2) Cal
$^4F_{3/2}$	875.0	1.461	1.268	875.0	1.463	1.435	875.0	1.467	1.641	875.0	1.454	1.359	875.0	1.452	1.231
$^2H_{9/2},^4F_{5/2}$	803.0	4.260	3.869	803.0	4.266	3.885	803.0	4.276	4.032	803.0	4.240	4.036	803.0	4.234	3.853
$^4S_{3/2},^4F_{7/2}$	747.0	3.911	3.588	741.6	3.680	3.579	743.0	3.332	3.536	743.4	4.102	3.899	741.2	4.104	3.797
$^4F_{9/2}$	682.0	0.687	0.269	682.2	0.462	0.215	683.4	0.236	0.264	684.4	0.466	0.279	682.4	0.763	0.270
$^4H_{11/2}$	625.8	0.154	0.068	628.8	0.117	0.066	629.0	0.135	0.067	623.4	0.387	0.070	625.2	0.466	0.068
$^2G_{7/2},^4G_{5/2}$	582.8	7.735	7.497	582.6	8.089	7.871	582.6	6.891	6.902	582.8	7.710	7.517	582.6	8.325	8.002
$^2K_{13/2},^4G_{7/2}$	525.4	1.438	1.428	525.2	1.704	1.520	525.4	1.244	1.559	525.6	1.980	1.485	525.4	2.103	1.442
$^4G_{9/2}$	512.6	0.522	0.499	512.6	1.023	0.534	512.6	0.830	0.578	512.2	0.354	0.526	512.2	0.587	0.493
$K_{15/2}, ^2G_{9/2}$	472.2	0.485	0.242	477.0	0.538	0.248	476.6	0.325	0.262	470.2	0.209	0.254	471.0	0.606	0.240
$^4G_{11/2},(^2D^2P)_{3/2}$	458.6	0.483	0.146	461.6	0.549	0.163	461.2	0.183	0.184	454.4	0.200	0.156	459.0	0.157	0.142
$^2P_{1/2},^2D_{5/2}$	429.6	0.621	0.167	430.8	0.313	0.196	430.8	0.091	0.230	427.6	0.896	0.181	429.0	0.765	0.181
Goodness of fit		0.114			0.098			0.040			0.136			0.214	

Bands	PD31 Wave-length (nm)	PD31 S(pm^2) Expt.	PD31 S(pm^2) Cal.
$^4F_{3/2}$	875.0	1.455	1.456
$^2H_{9/2},^4F_{5/2}$	803.0	4.244	4.275
$^4S_{3/2},^4F_{7/2}$	739.0	4.072	4.129
$^4F_{9/2}$	683.6	0.144	0.295
$^4H_{11/2}$	624.6	0.112	0.075
$^2G_{7/2},^4G_{5/2}$	582.4	6.374	6.427
$^2K_{13/2},^4G_{7/2}$	525.4	1.147	1.484
$^4G_{9/2}$	512.4	0.577	0.555
$^2K_{15/2}, ^2G_{9/2}$	471.0	0.031	0.268
$^4G_{11/2},(^2D^2P)_{3/2}$	457.0	0.078	0.167
$^2P_{1/2},^2D_{5/2}$	430.6	0.388	0.194
Goodness of fit		0.030	

and Ofelt[14] by treating them as induced electric-dipole transitions, pure ones being parity forbidden. The asymmetries produced by vibronic coupling of the central metal ion with its surrounding ions can induce electric-dipole transitions. These induced electric-dipole transitions can also occur due to the interaction of the central ion with the surrounding ions mixing into the $4f^n$ configuration states from configurations of opposite parity and thus relaxing the parity restriction. On this basis Judd and Ofelt expressed the electric-dipole line strength as a sum of products of phenomenological intensity parameters Ω_t and matrix elements of tensor operator $U^{(t)}$ connecting states of $4f^n$. The Judd-Ofelt approach is applicable to transition

Table 5. Slater Condon, landé, bonding and Racah parameters of Nd^{3+} ion doped borate and phosphate glass specimens

Parameters	Borate glass	Phosphate glass
F_2	325.435	330.874
F_4	45.472	42.514
F_6	4.922	5.185
landé		
ξ_{4f}	962.466	1012.960
Bonding		
β	0.983	0.999
$b^{1/2}$	0.093	0.021
Racah		
E^1	4793.222	4818.217
E^2	24.830	26.625
E^3	484.031	479.186

between Stark levels. For transition between J manifolds, the line strength has the simple form

$$S(J, J') = \sum_{t=2,4,6} \Omega_t < 4f^n \alpha SLJ \,||\, U^{(t)} \,||\, 4f^n \alpha' S'L'J' > 2 \quad (6)$$

where

$| 4f^n \alpha SLJ >$ are the basis states in the LS coupling scheme and α represents an extra quantum number that might be necessary to describe the states completely. The Ω_t parameters for a given ion-host combination are derived[6,15,16] from a least square fit of calculated and observed line strengths. The validity of the Judd-Ofelt treatment has been tested for most of the trivalent rare earths in crystals[17-19], liquids[20-26], powders[27] and glasses[3,5,28-37].

According to Judd-Ofelt[13,14], the oscillator strength of an electric-dipole transition between initial $| 4f^n \alpha SLJ >$ levels and terminal $| 4f^n \alpha' S'L'J' >$ levels of the rare earth ion is given by[38]

$$f_{JJ'} = 8\pi^2 mc/3h(2J+1)n\lambda \; \frac{(n^2+2)^2}{9} \; S(J, J') \quad (7)$$

Table 6. Judd-Ofelt parameters of Nd^{3+} ion doped borate and phosphate glass specimens

Specimen code	Judd-Ofelt (Ω_t) Parameters [pm^2]		
	Ω_2	Ω_4	Ω_6
BD02	7.278		
BD03	6.028		
BD05	9.142		
BD07	5.116		
BD08	4.309		
BD09	4.591		
BD11	4.599		
BD13	5.478		
BD14	4.338		
BD16	4.949		
PD18	7.139		
PD19	4.199		
PD21	7.627		
PD23	4.578		
PD24	4.354		
PD25	4.741		
PD26	4.655		
PD27	3.102		
PD29	4.534		
PD30	5.358		
PD31	3.177		

where

$S(J, J')$ (line strength) is given by Eqn (6). For Nd^{3+}, J=9/2 and the factor $(n^2+2)^2/9$ is the local field correction using the tight binding approximation.

From the experimentally observed spectra of the Nd^{3+} ion, the oscillator strength f_{expt} is calculated by the relation

$$f_{expt} = 4.318 \times 10^{-9} \int_{band} \varepsilon(\lambda)\, d\lambda \quad (8)$$

where

λ is the mean wavelength of the transition and $\varepsilon(\lambda)$ is the molar extinction coefficient.

Substituting the oscillator strength from Eqn (8) in Eqn (7) and applying the least-square fit method[16], using doubly reduced unit tensor

operator calculated in the intermediate coupling scheme, Ω_t parameters can be computed. These Ω_t parameters contain the effect of the odd-symmetry crystal field terms, radial integrals and energy denominators. Since the values for the unit tensor elements exhibit negligible change with host constituents, their values reported by Carnall[15,16] have been used.

The Ω_t parameters were computed[23] for each specimen by using least-square fit method taking into consideration all the absorption peaks observed. The values obtained are given in Table 6. Using these Ω_t values, the line strengths (S_c) have been calculated (Tables 3 and 4). The low values of goodness of fit between the so calculated S_c and measured S_m values show the applicability of Judd-Ofelt theory.

The Ω_2 parameter involves the long range terms in the crystal field potential and is most sensitive[39] to the local structural changes. For Nd^{3+}ion, the intensity of the $^4I_{9/2} \rightarrow {}^4G_{5/2}$, $^4G_{7/2}$ transition is the principal determiner of Ω_2. This transition satisfies the rule $|\Delta J| \leq 2$ and is known as hypersensitive transition. In general, the Ω_4 and the Ω_6 parameters for phosphate glasses are more than those for borate glasses.

In borate glasses (Table 6), when the primary modifier is changed from Li_2O to Na_2O, the values of parameters Ω_4 and Ω_6 increase, but when the secondary modifier is changed through MgO, CaO and BaO, it is observed that the value of Ω_4 parameter decreases while that of Ω_6 parameter increases. These changes in value of the parameters have a mixed effect on the laser parameters. When sensitizer CeO_2 is used as a codopant, it is observed that the change in Ω_6 parameter is more pronounced as compared to the change in Ω_4 parameter.

In phosphate glasses (Table 6), Na_2O has been used as the primary modifier for all specimens, while the secondary modifier is varied through MgO, CaO and BaO. The value of Ω_4 is found to increase, while that of Ω_6 decreases continuously. Sensitizers CeO_2 and $BiCl_3$ have been used as codopants. It has been observed that higher concentration of $BiCl_3$ produces the same effect as low concentration of CeO_2, suggesting the latter to be more efficient. CeO_2 produces an effect on Ω_4 and Ω_6 and similar to that in borate glasses.

3.3 Laser Parameters

Nd^{3+} ion is known to exhibit[40,41] transitions $^4F_{3/2} \rightarrow {}^4I_{9/2}$ (921 nm), $^4F_{3/2} \rightarrow {}^4I_{11/2}$ (1052-1057 nm) in phosphate glasses and 1054-1062 nm in borate glasses), $^4F_{3/2} \rightarrow {}^4I_{13/2}$ (1320-1370 nm) and $^4F_{3/2} \rightarrow {}^4I_{15/2}$ (1800 nm). For $^4F_{3/2} \rightarrow {}^4I_{11/2}$ transition, the effective line width of the peak fluoresence ranges[40] from 22 to 35 nm for phosphate glasses and from 34 to 38 nm for borate glasses. These spectral data and Judd-Ofelt parameters, given in Table 6, have been used for calculating various laser parameters.

3.3.1 *Spontaneous Emission Probability*

The spontaneous emission probability (A) from an initial manifold $|(S', L')J'>$ to final manifolds $|(\bar{S}, \bar{L})\bar{J}>$ is given by

$$A[(S',L')J'; (\bar{S}, \bar{L})\bar{J}] = \frac{64\pi^4 e^2}{3h(2J'+1)\lambda^3} n \cdot \frac{(n^2+2)^2}{9} \cdot S(J',\bar{J}) \quad (9)$$

where

$$S(J', \bar{J}) = \Omega_2 \, | U^{(2)}|^2 + \Omega_4 \, | U^{(4)}|^2 + \Omega_6 \, | U^{(6)}|^2$$

For Nd^{3+} ion J'=3/2 and the doubly reduced unit tensor operators reported by Krupke[6] have been used.

The A values for different transitions for the same specimen depend upon the emission wavelength, reduced matrix elements for the particular transition and the values of Ω_4 and Ω_6. It is interesting to note that A has maximum value (Table 7) for the transition $^4F_{3/2} \rightarrow {}^4I_{11/2}$, making this as the most probable laser transition. Since the values of A for $^4F_{3/2} \rightarrow {}^4I_{13/2}$ and $^4F_{3/2} \rightarrow {}^4I_{15/2}$ transitions are very small, it is not possible to observe them as laser transitions. The value of A for $^4F_{3/2} \rightarrow {}^4I_{9/2}$ transition suggests

that under suitable circumstances it can also appear as laser transition. The total value of spontaneous emission probability, A_T, for the $^4F_{3/2}$ state has been obtained by summing up A values for different transitions. This is used for calculating branching ratio for different transitions.

3.3.2 *Fluorescence Branching Ratio*

The fluorescence branching ratio (β) for transition from an initial manifold $|(S', L')J'>$ to final manifolds $|(\bar{S}, \bar{L})\bar{J}>$ is given by

$$\beta\,[(S', L')J'; (\bar{S}, \bar{L})\bar{J}] = \frac{A\,[(S', L')J'; (\bar{S}, \bar{L})\bar{J}]}{\sum_{\bar{S},\bar{L},\bar{J}} A\,[(S', L')J'; (\bar{S}, \bar{L})\bar{J}]} \quad (10)$$

where the sum is over all possible terminal manifolds. In the case of Nd^{3+} ion, the terminal manifolds are $^4I_{9/2}$, $^4I_{11/2}$, $^4I_{13/2}$ and $^4I_{15/2}$.

The β values depend upon Ω_4 and Ω_6, which, in their turn, depend upon glass composition. The value of β in the case of both borate and phosphate glasses is maximum for $^4F_{3/2} \longrightarrow {}^4I_{11/2}$ transition (Table 7). This shows the suitability of both borate and phosphate glasses to obtain laser action in near infrared region due to $^4F_{3/2} \longrightarrow {}^4I_{11/2}$ transition.

3 *Radiative Life Time*

The radiative lifetime (τ_R) is given by

$$\tau_R = \left[\sum_{\bar{S},\bar{L},\bar{J}} A\,[(S', L')J'; (\bar{S}, \bar{L})\bar{J}]\right] = A^{-1}_{\text{Total}} \quad (11)$$

where the sum is over all possible terminal manifolds ($^4I_{9/2}$, $^4I_{11/2}$, $^4I_{13/2}$ and $^4I_{15/2}$).

The radiative lifetime for a particular transition (τ) and radiative lifetime for the corresponding state (τ_R) are reciprocal of A and A_t respectively. The τ_R value for state $^4F_{3/2}$ and τ values for transitions $^4F_{3/2} \longrightarrow {}^4I_{9/2}$, $^4F_{3/2} \longrightarrow {}^4I_{11/2}$, $^4F_{3/2} \longrightarrow {}^4I_{13/2}$ and $^4F_{3/2} \longrightarrow {}^4I_{15/2}$ for both borate and phosphate glasses have been given in Table 7. Minimum τ values have been obtained for $^4F_{3/2} \longrightarrow {}^4I_{11/2}$ transition, suggesting it to be the most suitable laser transition.

3.3.4 *Stimulated Emission Cross-Section*

The stimulated emission cross-section (σ) for transition from an initial manifold $|(S', L')J'>$ to final manifolds $|(\bar{S}, \bar{L})\bar{J}>$ is expressed as

$$\sigma = \frac{\lambda_P^4}{8\pi c n^2 \Delta\lambda_{eff}} A\,[(S', L')J'; (\bar{S}, \bar{L})\bar{J}] \quad (12)$$

where

λ_P is the peak fluorescence wavelength of the emission band and $\Delta\lambda_{eff}$ is the effective fluorescence line width.

The rate of energy extraction from a laser material is dependent on the stimulated emission cross-section. Three methods have been used for its calculation based on (i) integrated absorption data and the Landenburg-Fuchtbaur equation using partial decomposition of the emission spectra into transition between individual Stark levels, (ii) Integrated absorption data and the Landenburg-Fuchtbaur equation using no decomposition and an average over all Stark levels from the initial and final J manifolds, and (iii) Judd-Ofelt intensity parameters.

The first two methods were used by Lempicki, *et al.*[42], while the third one was widely used by Weber, *et al.*[43], Tandon, *et al.*[30,32-35] and others[28,36,37,44,45].

The first method yields a higher value of σ, while the other two methods yield nearly equal values. Since an average over the Stark levels is more in the spirit of Judd-Ofelt approach, the radiative lifetime predicted by the last method is comparable with the experimental lifetime observed in the glass specimens with low concentration of Nd^{3+} ion having negligible quenching of fluorescence radiations.

The former BO_3 in borate glasses is known[46,47] to have a triangular structure, while PO_4 in phosphate glasses has a tetrahedral structure. This difference in structure is expected to

Table 7 : Laser parameters of Nd^{3+} ion doped borate and phosphate glass specimens for $^4F_{3/2}$ -> $^4I_{11/2}$ laser transition

Specimen code	Spontaneous emission probability A [s^{-1}]	Fluorescence branching ratio (β)	Radiative lifetime τ [μs]	Radiative quantum efficiency τ_R^* [μs]	Stimulated emission cross-section σ_p [pm^2]
BD02	1132-1158	0.486-0.509	863-883	429-440	1.942-2.288
BD03	1163-1190	0.495-0.520	840-859	426-437	2.000-2.358
BD05	955- 977	0.475-0.498	1023-1047	497-509	1.687-1.988
BD07	1151-1178	0.488-0.512	849-869	424-434	2.010-2.369
BD08	1233-1262	0.462-0.483	792-811	374-383	2.152-2.526
BD09	1222-1249	0.490-0.514	800-818	401-411	2.123-2.500
BD11	1213-1241	0.477-0.500	806-824	394-403	2.099-2.474
BD13	1254-1282	0.466-0.487	780-797	371-380	2.162-2.546
BD14	1238-1266	0.496-0.520	789-807	400-411	2.137-2.518
BD16	1282-1311	0.504-0.529	762-780	393-404	2.205-2.597
PD18	1185-1201	0.456-0.471	832-844	385-392	2.397-3.938
PD19	1243-1261	0.457-0.464	793-804	368-374	2.520-4.146
PD21	1187-1204	0.465-0.480	830-842	392-399	2.421-3.981
PD23	1283-1302	0.476-0.492	768-779	371-378	2.561-4.214
PD24	1266-1285	0.473-0.489	778-790	374-381	2.524-4.153
PD25	1253-1271	0.492-0.509	787-798	392-401	2.475-4.071
PD26	1238-1256	0.471-0.487	796-807	380-387	2.453-4.035
PD27	1268-1286	0.454-0.468	777-788	358-364	2.522-4.147
PD29	1322-1340	0.488-0.506	746-756	369-377	2.592-4.260
PD30	1270-1288	0.496-0.514	776-787	391-399	2.484-4.084
PD31	1401-1421	0.486-0.503	704-714	347-354	2.749-4.522

Radiative lifetime for state $^4F_{3/2}$

influence σ value. In general, the σ value for phosphate glasses has been found to be greater than that for borate glasses (Table 7).

The role of the modifier is very important for tailoring the stimulated emission cross-section. When two modifiers are used, one having higher percentage is known as the primary modifier and the other one as the secondary modifier. Usually, for the same valency of the modifier, σ increases with increase in the size of the cation. A systematic study[40] using alkali oxides as the primary modifier with P_2O_5 as glass former shows that the value of σ changes from 3.8 to 4.3 pm^2 in changing from lithium oxide to sodium oxide and it varies between 4.3 and 4.7 pm^2 for other alkali oxides. This shows that sodium oxide is a good primary modifier and has been used widely. The use of alkaline earth oxides instead of alkali oxides as primary modifier[40] gives a still poorer value of σ (2.0 to 3.5 pm^2). Consequently, lithium oxide was used for three specimens only, while sodium oxide was chosen as the primary modifier for the rest of the specimens. Increase in percentage of the primary modifier beyond a certain value does not further increase the σ value. Addition of the secondary modifier further increases the σ value. In the present work, MgO, CaO and BaO have been used as secondary modifiers. The σ values increase with the increase of the size of the cation of the modifier, viz., $MgO < CaO < BaO$.

Intermediates like Li_2O_3 and Al_2O_3 have been used to improve the quality of glass and to minimize the quenching effect of dopants. Al_2O_3 has been shown[40] to be better than Li_2O_3. Hence, Al_2O_3 has been used as an intermediate. Excess of intermediate lower the σ value. Decrease in percentage of intermediate Al_2O_3 from 29.73 to 14.78 shows an increase of 19 per cent in the value

of σ. This suggests that use of excessive amount of the intermediate lowers the σ values. Consequently, the percentage of the intermediate has been kept five per cent in all the specimens containing secondary modifiers.

It is well established[48] that high percentage of dopant results in quenching of the fluorescence radiation. It is found that percentage of dopant beyond 1.5 does not increase the σ value in the presence of the secondary modifier. Taking this fact into consideration, finally the percentage of Nd_2O_3 was kept at 1.45 per cent for both borate and phosphate glass specimens. Codopants like *Cr, Mn, Ce* and *Bi* have been used[49] to enhance the fluorescence of Nd^{3+}. CeO_2 and $BiCl_3$ have been shown[50,51] to be better than other codopants. Both of them were used in the present work. The use of CeO_2 increases the σ value by 3 per cent in calibo glass specimens (BD02,BD03) , by 5.6 per cent in borate glass specimens (BD07, BD09) and by 5-6 per cent in phosphate glass specimens (PD18, PD19 and PD29, PD31). In specimens PD25 and PD26, addition of 0.14 per cent $BiCl_3$ lowers value by 1 per cent, however, when its percentage is raised to 0.42, the σ value increases by 2 per cent (PD25, PD27). A comparative study of both these codopants shows that 0.42 per cent $BiCl_3$ increases σ by about 2 per cent, while 0.14 per cent CeO_2 increases σ by about 5-6 per cent. Thus, CeO_2 appears to be a better codopant in the role of sensitizer. Hence, it has been used for specimens BD16 and PD31.

Comparison of calculated σ values for borate and phosphate glasses with those reported[40] for silicate, fluoroberyllate and tellurite glasses (Fig. 4) shows that tellurite glasses are best and phosphate glasses the next best. However, tellurite glasses have low transmission in the desired region (near i.r.) due to high value of refractive index.

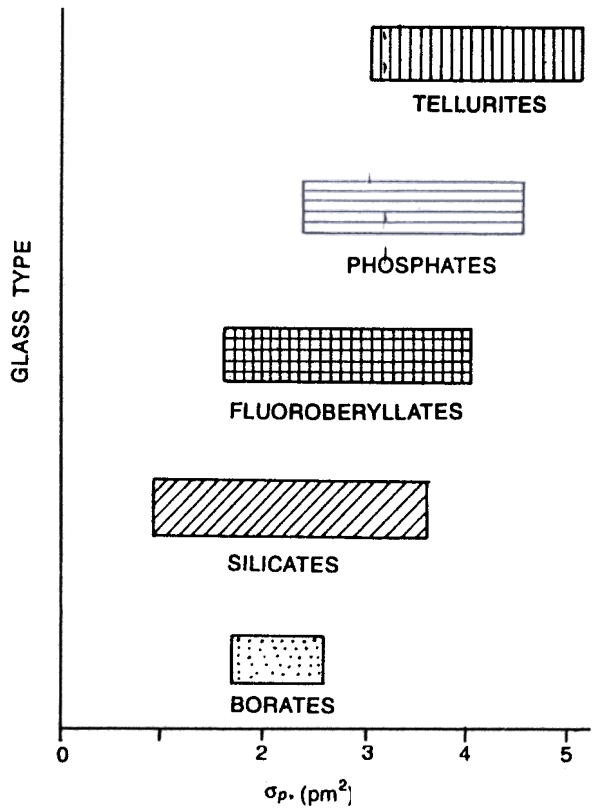

Figure 4. Range of stimulated emission cross-section for different neodymium doped glasses.

ACKNOWLEDGEMENT

The authors wish to acknowledge the financial support provided by the Aircraft System Panel, Aeronautical Research & Development Board, Ministry of Defence, Govt. of India. They are grateful to Dr M.P. Bhutra, Dr S.S.L. Surana, Dr K.K. Sule and Shri R.C. Govil for discussion.

REFERENCES

Kruegle, H.A. & Klein, L. High peak power output, high PRF by cavity dumping a Nd:YAG laser. *Applied Optics*, 1976, **15**, 466-71.

2. Northam, D.B.; Guerra, M.A.; Mack, M.E.; Itzkan, I. & Deradourian, C. High repetition rate frequency-doubled Nd:YAG laser for airborne bathymetry. *Applied Optics*, 1981, **20**, 968-71.

3. Reisfeld, R. & Jorgensen, C.K. Lasers and excited states of rare earths, Springer-Verlag Berlin Heidelberg, New York, 1977.

4. Snitzer, E.; Young, C.G. & Pressley, R.J.(Ed). Lasers; The chemical rubber co., cleveland, 1971, p 360.

5. Ebendorff-Heidepriem, H.; Seeber, W. & Ehrt, D. Spectroscopic properties of Nd^{3+} ions in phosphate glasses, *J. Non-Cryst. Solids*, 1995, **183**, 191-200.

6. Krupke, W.F., Induced-emission cross-sections in neodymium laser glasses. *IEEE J. Quantum Electron.*, 1974, **QE-10**, 450-57.

Quenching Media, Metals Handbook, Pt IV. American Society for Metals, Metals Park, Ohio, 1981, p.615.

8. Wong, E.J. Configuration interaction of the Pr^{3+} ion, *J. Chem. Phys.*, 1963, **38**, 976-78.

9. Wong, E.J. Tayler series expansion of the intermediate coupling energy levels of Nd^{3+} and Er^{3+}, *J. Chem. Phys.*, 1961, **35**, 544-46.

10. Dieke, G.H. Spectra and energy levels of rare earth ions in crystals. InterScience, John Wiley and Sons, New York, 1968.

11. Tandon, S.P. & Mehta, P.C. Spectral intensities of Pr^{3+} β-diketonates, *J. Chem. Phys.*, 1970, **52**, 4313-15.

12. Sharma, Y.K. Spectral and electral properties of lanthanide ions in different environment, University of Jodhpur, Jodhpur, India, 1991! PhD thesis.

13. Judd, B.R. Optical absorption intensities of rare-earth ions, *Phys. Rev.*, 1962, **127**, 750-61.

14. Ofelt, G.S. Intensities of crystal spectra of rare-earth ions, *J. Chem. Phys.*, 1962, **37**, 511-20.

15. Goublen, C.H. Method of statistical analysis. Asia Publishing House, Bombay, 1964. p.134.

16. Carnall, W.T. Fields, P.R. & Rajnak, K. Electronic energy levels in the trivalent lanthanide aquo ions I Pr^{3+}, Nd^{3+}, Pm^{3+}, Sm^{3+}, Dy^{3+}, Ho^{3+}, Er^{3+}, Tm^{3+}. *J. Chem. Phys.*, 1968, **49**, 4424-442.

17. Tandon S.P., Surana, S.S.L., Tandon, K., Bhutra, M.P., Sule, K.K., Govil, R.C., Bishnoi, N.B., & Sharma, Y.K., Optical studies of rare-earth lasing materials suitable for higher repetitive rates with special reference to defence applications. AR & DB Project No. 393, 1989.

18. Leavitt, R.P. & Morrison, C.A. Crystal field analysis of triply ionized rare-earth ions in lanthanide trifluoride-II, Intensity Calculations. *J. Chem. Phys.*, 1980, **73**, 749-57.

19. Jorgensen, C.K. & Reisfeld, R. Judd-Ofelt parameters and chemical bonding. *J. Less-Common Met.*, 1983, **93** 107-112.

20. Mason, S. F.; Peacock, R. D. & Stewart, B. Ligand-polarization contributions to the intensity of hypersensitive trivalent lanthanide transition. *Molecular Physics*, 1975, **30**, 1829-841.

21 Foster, D.R.; Richardson, F.S. & Schwartz, R.W. Optical spectra and crystal field analysis of Sm in the cubic Cs NYCl host. *J. Chem. Phys.*, 1985, **82**, 618-631.

22. Tandon, S.P. & Mehta, P.C. Bonding inferred from study of nephelauxetic effect in praseodymium complexes. Spectry. Letters, 1969, **2**, 255-59.

23. Mehta, P.C. & Tandon, S.P. Spectral intensities of some Nd^{3+} β-diketonates. *J. Chem. Phys.*, 1970, **53**, 414-17.

24. Surana, S.S.L.; Mathur, R.C. & Tandon, S.P. Spectral study of aprotic Pr^{3+} and Nd^{3+} laser liquids : interaction parameters, bonding and Judd-Ofelt intensity parameters. *J. Phys. Chem.*, 1975, **8**, 2323-328.

25. Tandon, S.P. & Vaishnava, P.P. Rare-earth aromatic acid complxes: Electrostaic interaction, bonding and Judd-Ofelt intensity parameters. *Can. J. Spectroscopy*, 1977, **22**, 17-21.

26. Tandon, S.P.; Sharma, Y.K.; Bishnoi, N.B. & Surana, S.S.L. Spectoscopic studies of Nd^{3+} ternary amino acid complexes, *Rev. Tec. Ing. Univ. Zulia*, 1991, **14**, 169-72.

27 Tandon, S.P.; Gokhroo, A.; Surana, S.S.L.; Bhutra, M.P. & Tandon, K. Spectral intensities inferred from diffuse reflectance spectra of lanthanide complexes in the form of solid-solid solutions. *J. Chem. Phys.*, 1987, **86**, 7243-244.

28. Stokowski, S.E.; Saroyan, R.A. & Weber, M.J. Nd-doped laser glass spectroscopy and physical

properties. Lawrence livermore National Laboratory, USA, 1981. Report M-095.

29. Weber, M.J. Fluorescence and glass lasers. *J. Non-Cryst. Solids*, 1982, **47**, 117-34.

30. Sharma, Y.K.; Bishnoi, N.B.; Surana, S.S.L. & Tandon, S.P. Spectral studies of Pr^{3+}, Sm^{3+} and Ho^{3+} ions in sodium barium borate glass. *J. Pure Appl. Phys.*, 1992, **4**, 200-211.

31. Bishnoi, N.B.; Sharma, Y.K.; Surana, S.S.L. & Tandon, S.P. Electrical and optical study of Cr^{3+} doped chlorophosphate and phosphate glasses. 1993, **57**, 5088-93.

32. Sharma, Y.K.; Mathur, S.C.; Dube, D.C. & Tandon, S.P. Optical absorption spectra and energy band gap in praseodymium borophosphate glasses. *J. Mat. Sci. Lett.*, 1995, **14**, 71-73.

33. Tandon, S.P.; Sharma, Y.K.; Bishnoi, N.B. & Surana, S.S.L. Dependance of fluorescence spectra of Pr^{3+} doped chlorophosphate glasses on doping concentration. *Sing. J. Phys.*, 1995, **11**, 93-97.

34. Sharma, Y.K.; Dube, D.C. & Tandon, S.P. Spectral studies of Pr^{3+} doped borophosphate glass. *Mat. Sci. Forum*, 1996, **223**, 105-108.

35. Sharma, Y.K.; Mathur, S.C.; Dube, D.C. & Tandon, S.P. Electrical and optical band gap studies in neodymium borophosphate glasses. *J. Mat. Sci. Lett.*, 1996, **15**, 1054-56.

36. Quimby, R.S. & Miniscalco, W.J. Modified Judd-Ofelt technique and application to optical transitions in Pr^{3+} doped glass. *J. Appl. Phys.*, 1994, **75**, 613-15.

37. Medeiros Neto, J.A.; Hewak, D.W. & Tate, H. Application of a modified Judd-Ofelt theory to praseodymium doped fluoride glasses. *J. Non-Cryst. Solids*, 1995, **183**, 201-207.

38. Jacobs, R.R. & Weber, M.J. Dependence of the $^4F_{3/2} \longrightarrow {}^4I_{11/2}$ induced emission cross-section for Nd^{3+} on glass composition. *IEEE J. Quantum Electron.*, 1976, **QE-12**, 102-11.

39. Bhatia, B.; Bhutra, M.P. & Tandon, S.P. Spectroscopic study of Pr^{3+} amino acid ternary complexes in aqueous solutions. *Rev. Tec. Ing. Univ. Zulia*, 1988, **11**, 69-72.

40. Weber, M.J. & Wiss. Z. Oxide and halide laser glasses, Friedrich-Schiller-Univ. Jena, Math. Naturwiss R., 1983, **32**, 239-50.

41 Jezowska-Trzebiatowska, B.; Ryba- Romanowski, W.; Mazurak, Z. & Bubietynska, K., Radiative transition probabilities within 4f configurations of Nd^{3+} and Er^{3+} in $PoCl_3$:$ZrCl_3$. *Chem. Phys. Lett.*, 1976, **43**, 417-19.

42. Lempicki, A.; Klein, R.M. & Chinn, S.R. Spectroscopy and lasing of a high Nd^{3+} concentration Al-phosphate glass. *IEEE J. Quantum Electron.*, 1978, **QE-14**, 283-93.

43. Weber, M.J.; Saroyan, R.A. & Ropp, R.C. Optical properties of Nd^{3+} in metaphosphate glasses. *J. Non-Cryst. Solids*, 1981, **44**, 137-48.

44. Lakshman, S.V.J. & Suresh, A.K. Spectral absorption properties of Pr^{3+}, Nd^{3+}, Er^{3+} and Tm^{3+} ions in zinc sodium phosphate glass. *Phys. and Chem. Glasses*, 1988, **29**, 146-49.

45. Lakshman, S.V.J. & Suresh, A.K., Evaluation of spectroscopic parameters for Pr^{3+} ions in potassium zinc sulphate glass. *J. Non-Cryst. Solids*, 1986, **85**, 162-69.

46. Silver, A.H. & Bray, P.J. Nuclear magnetic resonance absorption in glass I. Nuclear quadrupole effects in boron oxide, soda boric oxide and borosilicate glasses. *J. Chem. Phys.*, 1958, **29**, 984-90.

47. Wong, J. & Angell, C.A. Glass structure by spectroscopy. Marcel Dekker, New York, 1976.

48. Weber, M.J. Hand book of physics and chemistry of rare-earths, Vol IV; Gschneidner, K.A., Jr. and Eyring, L. (Eds). North-Holland Publishing Company, Amsterdam, 1979. p.275.

49. Van Uitert, L.G. Luminescence of inorganic solids. Academic press, New York, 1966. p.465.

50. Gandy, H.W.; Ginther, R.J. & Weller, J.F. Energy transfer in silicate glass coactivated with cerium and neodymium. *Phys. Lett.*, 1964, **11**, 213-14.

Contributors

Prof SP Tandon obtained his PhD from Agra University in 1964. He has published 190 research papers on molecular and lanthanide spectroscopy, LCAO-MO calculations, materials science and laser physics. He visited and worked at universities in Dortmund and Gotingen (West Germany), Tronheim (Norway), Upsala (Sweden), Paris and Strassburg (France), Zurich (Switzerland), International Centre for Theoretical Physics (Italy). He also worked as educational expert to Government of Iraq (University of Sulaimaniyah).

Dr YK Sharma is working as Assistant Professor of Physics at JNV University, Jodhpur. He obtained his PhD from University of Jodhpur in 1991. He has published 40 papers on lanthanide spectroscopy and laser materials. He has worked as Research Fellow for Aeronautical Research & Development Board projects. He was awarded Young Scientist Project on study and development of lanthanide doped glasses for laser and LSC's (1991-1994) by Government of India, Department of Science and Technology, New Delhi.

Dr NB Bishnoi is working as Lecturer in Physics, Government Nehru Degree College, Jhajhar. He obtained his PhD from University of Jodhpur in 1991. He has published 25 papers on lanthanide spectroscopy and laser materials. He has worked as Research Fellow for Aeronautical Research & Development Board projects.

Dr (Mrs) K Tandon is Associate Professor of Chemistry at JNV University, Jodhpur. She obtained her PhD from University of Jodhpur in 1967. She has published 60 research papers on cordination chemistry, isotopic substitution and laser materials. She visited and worked at universities of Dortmund and Gotingen (West Germany), Tronheim (Norway), Upsala (Sweden), Paris and Strassburg (France), Zurich (Switzerland) and International Centre for Theoretical Physics (Italy).